Transactions on Engineering and Technology Research
ISSN: 2960-1797, eISSN: 2960-2246 | Volume 1
AMMEE 2023

Kinematic Analysis and Control Study of a 3-DOF Harvesting Robot

Jinghao Hu*

College of Mechanical Engineering, North China Electric Power University, China

* Corresponding Author E-mail: hjh19518088582@163.com

Abstract. In this paper, a three-degree-of-freedom harvesting robot is proposed and its feasibility for harvesting fruit from shorter plants is verified, although agricultural robots are widely used in various agricultural production activities, there is a lack of adequate analysis in this field. The kinematic analysis is carried out and the kinematic parameters and trajectory equations of the manipulator are determined. A control method of the manipulator's arm based on fuzzy neural network control is proposed, and its feasibility is verified by Matlab through working range analysis and error test. Our goal is to improve the efficiency, convenience, and cost-effectiveness of harvesting dwarf crops by studying this small harvesting robot.

Keywords: robot manipulator, kinematic analysis, kinematic control, fuzzy theory, ANFIS network.

1. Introduction

With the continuous development of robot and robotic arm technology, their application in fields such as manufacturing and healthcare is becoming increasingly widespread. As high-precision and high-degree-of-freedom robots, robotic arms have the advantages of high precision, good stability, diversified functions, and a high degree of automation[1], thus they are receiving more and more widespread applications. In the manufacturing industry[2], robots have replaced human labor in some industrial processes, greatly improving work efficiency and production efficiency. In the healthcare industry, the application of robotic arms is also becoming increasingly widespread. For instance, Steven Dingert's team[3] has developed remotely controlled surgical robots capable of performing low-risk, high-precision surgeries in a short period. In the field of kinematics, Kazunori Shinohara [4] has utilized robotic arms to simulate the kinematics of swimmers, to improve their skills and performance.

Apart from the aforementioned applications, as the mechanization level in agriculture continues to increase, robotic arms are increasingly replacing traditional manual labor. For example, Kai Li's team[5] has simulated and analyzed the efficacy of robotic arms in kiwi fruit pollination, achieving a success rate of 85% with lightweight pollination robotic arms. Yafei Li[6] has used deep gradient control algorithms to achieve trajectory control of harvesting robotic arms. Wang Shuo's team[7] has applied a vision-based autonomous navigation system to agricultural robots, enabling them to operate independently in orchards. Li Hailong[8] significantly improved the spraying accuracy of agricultural robotic arms by using a combined error adjustment approach. Ingrid J. Moreno[9] used Simulink and Qube-Server platforms to simulate path tracking of off-road agricultural robots, obtaining optimal path solutions and reducing experimental costs and time. Ørum Jens Erik[10] and his team successfully conducted crop rotation experiments with robotic arms in the high-tech farms of Oldambt, Netherlands. Xizhi Wu[11] reduced the repeated work area of agricultural robots by 38.54% and the number of work cycles by 35% through Complete Coverage Path Planning (CCPP) technology. From the above examples, it can be seen that robotic arms have become a core technology in agriculture and have a significant impact on agricultural production.

Due to extensive research on robotic arms, researchers have adopted different technical approaches and methods for different parts and applications of robotic arms. Sandeep Kumar[12] designed a four-wheel skid-steer mobile platform and a Cartesian serial (PPP) robotic arm, simulated using Solidworks and ADAMS software and controlled using a six-channel RF controller. Rajeev

Content from this work may be used under the terms of CC BY-NC 4.0 licence (https://creativecommons.org/licenses/by-nc/4.0/).
Published by Warwick Evans Publishing.

Agrawal's team[13] evaluated system stability using PID control combined with the transfer function of the control system. H. Kareemullah and D. Najumnissa[14] remote-controlled robotic arms, using wifi wireless technology to control motor movement and ultimately control the robotic arm. However, due to the difficulties in precisely controlling multi-degree-of-freedom robotic arms, Namhyun Kim[15] proposed a Disturbance Observer-based Dual-Position Feedback (DOB-DPF) controller to improve positioning accuracy by real-time compensation for deviation using only one internal sensor. Additionally, Jinxiao Gao's team[16] used a Kinect visual image sensor to recognize human skeleton data and identify and control the operator's movements for a 4-DOF robotic arm. Chuanyang Li[17] studied a manipulator designed with N double-tripod multi-loop modules to achieve multi-mode control of the target manipulator. Ranjeet Ranjan[18] used Matlab simulation technology to create block and robot models of a humanoid arm and demonstrated the geometric model and motion of a 3-DOF double linkage arm. From the above examples, it can be seen that the research methods of robotic arms mainly include PID, remote control, Matlab/Simulink modeling, and dynamic analysis methods. These methods are used to achieve control of robotic arms under different operating states.

In previous research reports, there have been few studies on harvesting agricultural robots for shorter plants (less than 1 meter in height). To improve the efficiency of harvesting fruits from these types of plants, this paper designs a three-degree-of-freedom harvesting mechanical arm and proposes a control method. Section 2 analyzes the kinematics of the arm and derives equations for each link. In Section 3, a fuzzy-based ANFIS network control method is proposed and tested for errors. The arm is shown to be capable of efficiently harvesting shorter plants' fruits in various scenarios.Fig.1 illustrates the main structure and operation of the robot.

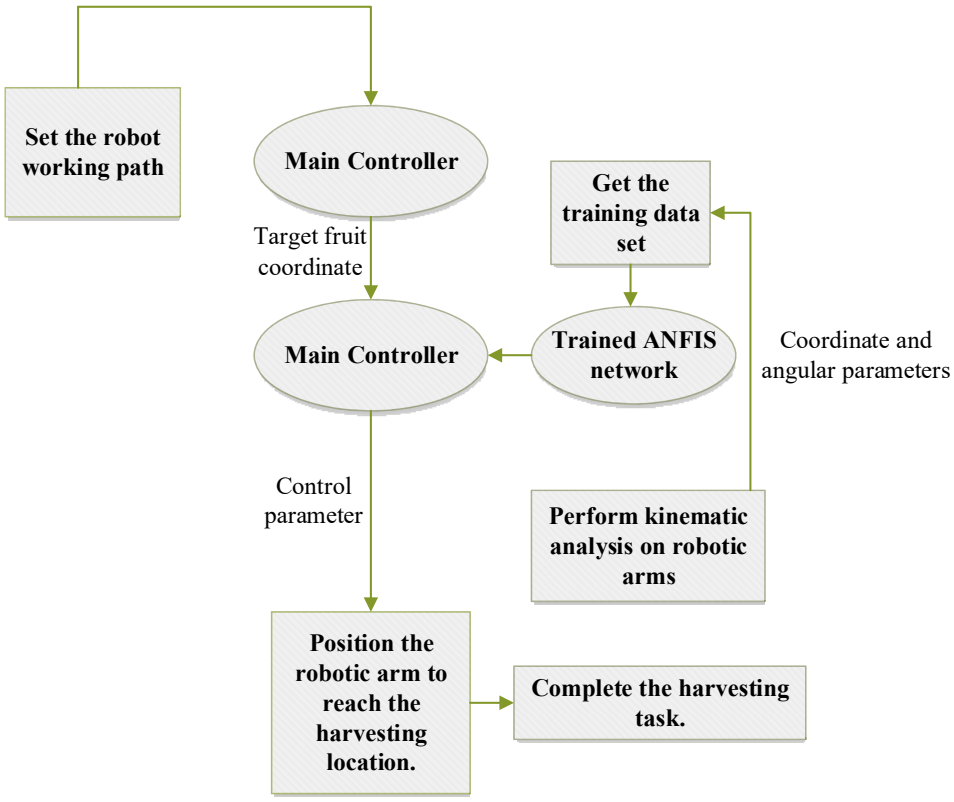

Fig.1 Main structure and operation of the robot.

2. Theoretical analysis

During the pollination process of the harvesting robotic arm, it is necessary for the gripping claws of the arm to reach any position as much as possible and to perform the pollination operation in order according to the position and direction of the target fruit. We chose a 3-degree-of-freedom articulated robotic arm for the harvesting arm, and the structure of the robotic arm is shown in Table 1.

Table 1. Main components of the robot

Number	Name	Function
1	Chassis	Robotic Arm Base
2	Base Coordinate Origin	Coordinate Localization Origin
3	Link1	First Section of Robotic Arm
4	Link2	Second Section of Robotic Arm
5	Gripping Claw	Picking Fruits
6	Target Recognition Processor	Identifying and Locating Fruits
7	Main Controller	Controlling Robotic Arm Movement
8	Fruit Box	Storing picked fruits
9	Target fruit	Mechanical arm gripping target

The working diagram of the target fruit harvesting robotic arm is shown in Fig.2. The robotic arm consists of a wheeled chassis, mechanical arm, gripping hand, and positioning system. The target recognizer can take real-time photos to identify ripe fruits, using the principle of disparity imaging to obtain the three-dimensional coordinates of the flower in the visual system. After obtaining the three-dimensional coordinates of the target fruit in the visual system, it is converted into three-dimensional coordinates of the robotic arm operating system and then sent to the main controller to drive the robotic arm for pollination.

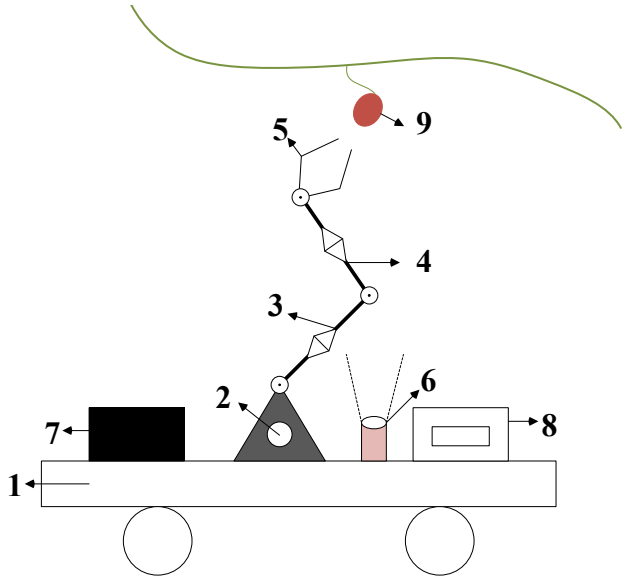

Fig.2 Schematic diagram of the overall operation of the harvesting robot.

Before simulating the robotic arm's motion control, we need to derive the forward and inverse kinematics formulas, which are used to determine the robot's end position and joint angles, respectively. The forward kinematics formula uses rotation and position transformations to obtain the end position, given the joint angles. In contrast, the inverse kinematics formula derives the joint angles from the end position and is primarily used for position control. Kinematic analysis is essential for trajectory planning and motion control.

Forward kinematic analysis: The 3-DOF robotic arm has three links that can rotate around a given axis, as shown in Fig.3. Kinematic analysis can be used to determine the position and orientation of the end effector of the robotic arm.

Firstly, we use the D-H parameter method to describe the linkage relationship of the robotic arm. According to the physical parameters given in Table 2, we know that the link lengths of the robotic arm are l_1,$l_2$and l_3.

Table 2. Physical parameters of the components of the robotic arm.

Name	Length[mm]	Wight [kg]
Link1	400	0.45
Link2	400	0.45
End effector	220	0.35
Link3	110	0.20
Gripping hand claws	110	0.15

The working principle and coordinate system of the 3-DOF robotic arm are shown in Fig.3. The robotic arm has three active joints, and its end is equipped with a gripper.

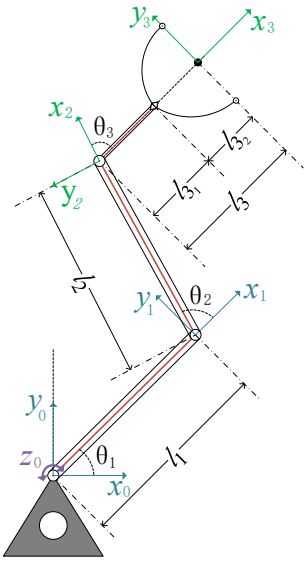

Fig.3. Schematic Diagram of the Working Principle of the Robotic Arm.

Next, we will compute the transformation matrices for each link using the D-H parameter method, and based on the D-H parameters provided in Table 3, we obtain the following transformation matrices.

Table 3 parameters of the robotic arm.

i	α_{i-1}	a_{i-1}	d	θ
1	0°	l_1	0	θ_1 $(0\sim\frac{\pi}{2})$
2	0°	l_2	0	θ_2 $(0\sim\frac{\pi}{2})$
3	0°	l_3	0	θ_3 $(0\sim\pi)$

Where the variables mean:

α_{i-1}: angle of rotation around the z-axis.

θ: angle of rotation around the x-axis.

a_{i-1}: distance between the z-axes along the x-axis direction.

d: distance between the x-axis along the z-axis direction.

The transformation matrix for the first link (from coordinate system 0 to coordinate system 1) is:

$$ {}^{0}_{1}T = \begin{bmatrix} c1 & -s1 & 0 & l_1c1 \\ s1 & c1 & 0 & l_1s1 \\ 0 & 0 & 1 & 0 \\ 0 & 0 & 0 & 1 \end{bmatrix} \tag{1} $$

The transformation matrix for the second and third links is as follows:

$$ {}^{1}_{2}T = \begin{bmatrix} c2 & -s2 & 0 & l_2c2 \\ s2 & c2 & 0 & l_2s2 \\ 0 & 0 & 1 & 0 \\ 0 & 0 & 0 & 1 \end{bmatrix} \tag{2} $$

$$ {}^{2}_{3}T = \begin{bmatrix} c3 & -s3 & 0 & l_3c3 \\ s3 & c3 & 0 & l_3s3 \\ 0 & 0 & 1 & 0 \\ 0 & 0 & 0 & 1 \end{bmatrix} \tag{3} $$

Next, we multiply these three transformation matrices together to obtain the forward kinematics transformation matrix for the entire robotic arm${}^{0}_{3}T$:

$$ {}^{0}_{3}T = {}^{0}_{1}T\,{}^{1}_{2}T\,{}^{2}_{3}T \tag{4} $$

By performing the calculations, we can obtain a 4×4 matrix that contains both position and orientation information${}^{0}_{3}T$:

$$ {}^{0}_{3}T = \begin{bmatrix} g_x & f_x & m_x & n_x \\ g_y & f_y & m_y & n_y \\ g_z & f_z & m_z & n_z \\ 0 & 0 & 0 & 1 \end{bmatrix} = \begin{bmatrix} R_{3\times3} & P_{3\times1} \\ 0_{1\times3} & 1 \end{bmatrix} \tag{5} $$

In this equation:$R_{3\times3}$ is the Manipulator attitude;$P_{3\times1}$ is the position of the Manipulator.

Obviously, the position and orientation of the end effector, which is the gripper of the harvesting robotic arm, are directly influenced by the motion states of each joint. Thus, we can express it as:

$$ \begin{cases} g_x = c3(c1c2 - s1s2) - s3(c1s2 + c2s1) \\ g_y = c3(c1s2 + c2s1) + s3(c1c2 - s1s2 \\ g_z = 0 \\ f_x = -c3(c1s2 + c2s1) - s3 * (c1c2 - s1s2) \\ f_y = c3(c1c2 - s1s2) - s3 * (c1s2 + c2s1) \\ f_z = 0 \\ m_x = 0 \\ m_y = 0 \\ m_z = 2 \\ n_x = c1l_1 - l_3s3(c1s2 + c2s1) + c1c2l_2 - l_2s1s2 + c3l_3(c1c2 - s1s2) \\ n_y = l_1s1 + l_3s3(c1c2 - s1s2) + c1l_2s2 + c2l_2s1 + c3l_3(c1s2 + c2s1) \\ n_z = 0 \end{cases} \tag{6} $$

Inverse kinematics analysis calculates joint displacement and rotation based on the end effector's position and orientation. Through a system of equations using forward kinematics, we can solve for these joint values.

Calculate the x and y coordinates of the gripping point of the gripper claw:

$$ x = l_1 * cos\theta_1 + l_2 * cos(\theta_1 + \theta_2) + l_3 * cos(\theta_1 + \theta_2 + \theta_3) \tag{7} $$

$$ y = l_1 * sin\theta_1 + l_2 * sin(\theta_1 + \theta_2) + l_3 * sin(\theta_1 + \theta_2 + \theta_3) \tag{8} $$

The polar angle θ of the gripping claw relative to the base coordinate system can be calculated using the following formula:

$$ \theta = \arctan(y, x) \tag{9} $$

Calculate the rotation angle of the first joint θ_1:

The distance D from the first joint to the end effector can be calculated based on the x and y coordinates of the gripping point of the gripping claw and the length l_3 of the third arm, as shown below:

$$D = \sqrt{x^2 + y^2 - {l_3}^2} \tag{10}$$

Then, the angle of the first joint can be calculated using inverse trigonometric functions θ_1:

$$\theta_1 = \arctan(y, x) - \arctan(l_3, D) \tag{11}$$

Calculate the rotation angle of the second joint θ_2:

The angle θ_{23} between the second and third joints and the distance R from the second joint to the end effector can be calculated simultaneously using the cosine and sine laws, as shown below:

$$R = l_1 * \cos(\theta_{23}) + l_2 * \cos(\theta_{23} + \theta_2) \tag{12}$$

The rotation angle of the second joint can be calculated using inverse trigonometricfunctions:

$$\theta_2 = \arctan(\sin\theta_{23}, cos\theta_{23}) - \arctan(R\sqrt{1 - sin^2\theta_3}, Rcos\theta_3) \tag{13}$$

Finally, the rotation angle of the third joint can be calculated using the following formula θ_3:

$$\theta_3 = \arctan\left(\sqrt{1 - sin{\theta_3}^2}, cos\theta_3\right) - \arctan\left(\sqrt{1 - sin{\theta_2}^2}, cos\theta_2\right) \tag{14}$$

$\sin\theta_2$ and $\sin\theta_3$ can be obtained from the previous calculations.

3. Simulation Analysis and Validation

We can use Matlab software with fuzzy control theory to simulate and analyze a three-degree-of-freedom three-link manipulator. Firstly, we establish the geometric model and dynamic model of the manipulator based on Fig.3 and the analysis mentioned above. The geometric model describes the external shape and rod relationships of the manipulator, while the dynamic model describes its kinematic and dynamic characteristics. However, these models alone are insufficient for motion control, and a control model needs to be developed on this basis. Here, we employ the concept of fuzzy control to establish a fuzzy controller for controlling the manipulator. During the process of simulation analysis, we can optimize and adjust the control algorithm, kinematics, and dynamic parameters of the manipulator as needed. By evaluating and validating the control strategy of the manipulator through simulation results and data analysis, we can provide a scientific basis for practical applications and development.

Fuzzy control theory is a control method based on fuzzy mathematics and control principles. It has advantages over traditional precise control methods, including strong robustness and adaptability, simplicity and ease of implementation, human-machine interaction, and the ability to balance performance and stability.

By using fuzzy logic, we can develop a straightforward fuzzy reasoning system to deduce inverse kinematics, eliminating the need for complex analytical solutions. Below is a brief introduction and detailed explanation of this development process.

The forward kinematics formula of a three-degree-of-freedom robotic arm is used to calculate coordinates (x,y) within a range of rotation angles. These coordinates serve as training data for an ANFIS(adaptive neuro-fuzzy inference system) network. The ANFIS network learns how to map coordinates (x,y) to joint angles ($\theta_1, \theta_2, \theta_3$) and is employed for controlling the robotic arm. The control system utilizes the trained ANFIS network to infer joint angles and apply forces, thereby moving the robotic arm to the desired position.

In Fig. 4, the positions that the robotic arm can reach in space under certain conditions controlled by the ANFIS network are presented. Different values of ($\theta_1, \theta_2, \theta_3$) will affect the coordinates of the

end effector. In the following content, we will establish the mapping relationships between all landing point (*x*,*y*) coordinates and $(\theta_1, \theta_2, \theta_3)$, and apply them to the control system.

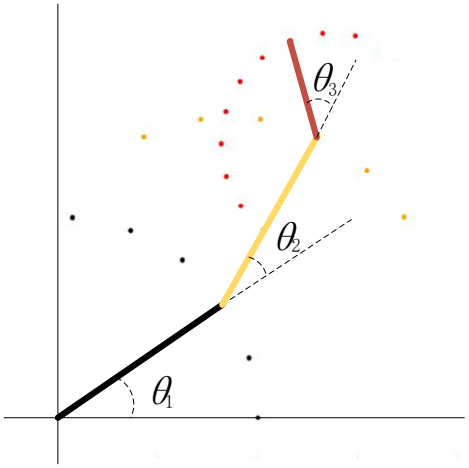

Fig.4 Some combinations of possible $\theta_1, \theta_2, \theta_3$ are shown.

First, we will generate training data. Using the information provided earlier, we can determine the coordinates (*x*,*y*) of the end effector for each combination of $(\theta_1, \theta_2, \theta_3)$ using forward kinematics. Using Matlab, we can generate data for all combinations of $(\theta_1, \theta_2, \theta_3)$ and save them in a matrix as training data. We can then visualize the coordinates of the final grasp point for all combinations in Fig.5.

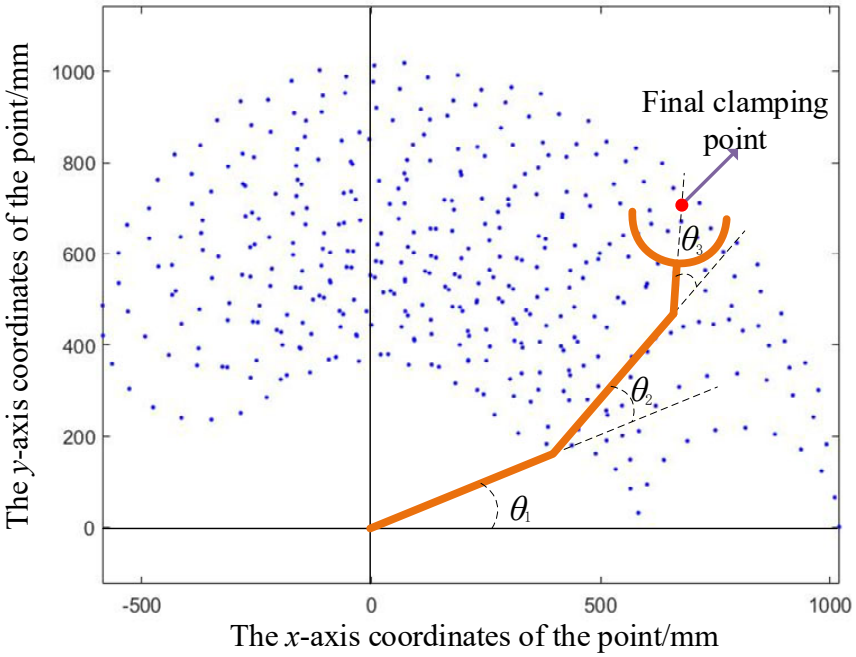

Fig.5 The coordinates of all possible landing points of the clamping point.

Furthermore, in Fig.6, the potential coordinates of the endpoints of Link1 and Link2 will be provided. These coordinates will be labeled in Fig.6(a) and Fig.6(b), respectively, serving as validation data for training the ANFIS network.

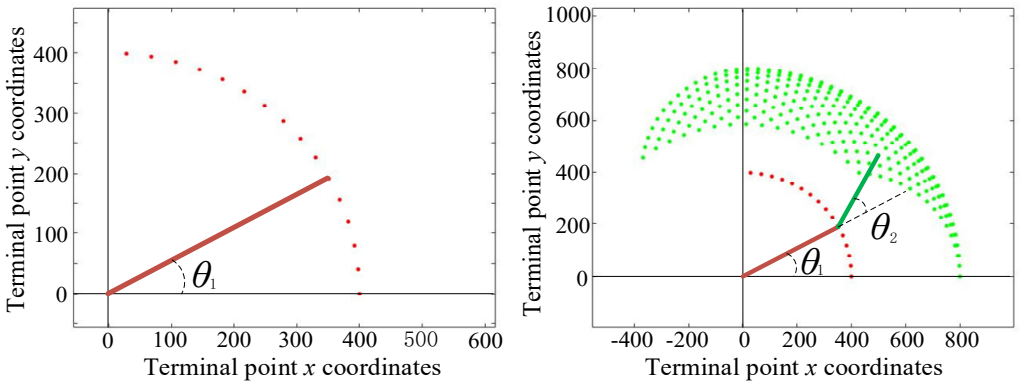

Fig.6 The endpoint positions of the remaining components. (a)Terminal coordinates of Link1. (b)Terminal coordinates of Link2.

One approach to constructing an ANFIS solution for this problem is to build three separate ANFIS networks, each responsible for predicting $\theta_1, \theta_2, \theta_3$.

To train the ANFIS network for angle prediction, we need to use sample input-output data. The first ANFIS network takes x and y coordinates as input and the corresponding θ_1 value as the output for training. data1 contains the x-y-θ_1 dataset required to train the first ANFIS network. Therefore, data1 will be used as the dataset for training the first ANFIS network.

Accordingly, data2 and data3 will be used as the datasets for training the second and third ANFIS networks, respectively.

Once trained, the three ANFIS networks have learned to approximate the angles $(\theta_1, \theta_2, \theta_3)$ as a function of the coordinates (x, y). One advantage of using the fuzzy method is that ANFIS networks can approximate the angles of coordinates that are similar but not the same as the training coordinates. For example, the trained ANFIS networks can now approximate the angles of coordinates between two points, even if these points are not present in the training dataset. This allows the final controller to smoothly move the robotic arm in the input space.

Now, the trained ANFIS networks need to be integrated with the control system of the robotic arm to control its motion. This requires real-time feedback of the robotic arm's position and making the necessary adjustments. The ultimate goal is to achieve accurate control of the robotic arm to perform different tasks. However, before formal deployment, an important step is to validate the networks to determine their performance in a larger control system. Since this example deals with a three-joint robotic arm, its inverse kinematics formula can be derived, making it possible to test the answers generated by the ANFIS networks against the answers derived from the formula. According to Fig.5, the main working area of the robotic arm is within the range $-200 < x < 400$ and $500 < y < 700$. For testing purposes, a specific region within the range $0 < x < 1$ and $500 < y < 501$ can be selected.

The $(\theta_1, \theta_2, \theta_3)$ values predicted by the trained ANFIS networks are obtained by evaluating the ANFIS for a given input using the command evaluation. Here, the FIS outputs for the same x-y values used in the inverse kinematics formula are obtained by using the evaluation values. The evaluation values and the values obtained from the actual kinematic solution are compared to validate the accuracy of the ANFIS networks. The simulation training and evaluation verification of the ANFIS networks can be performed using Matlab, and the resulting errors are shown in Fig.7.

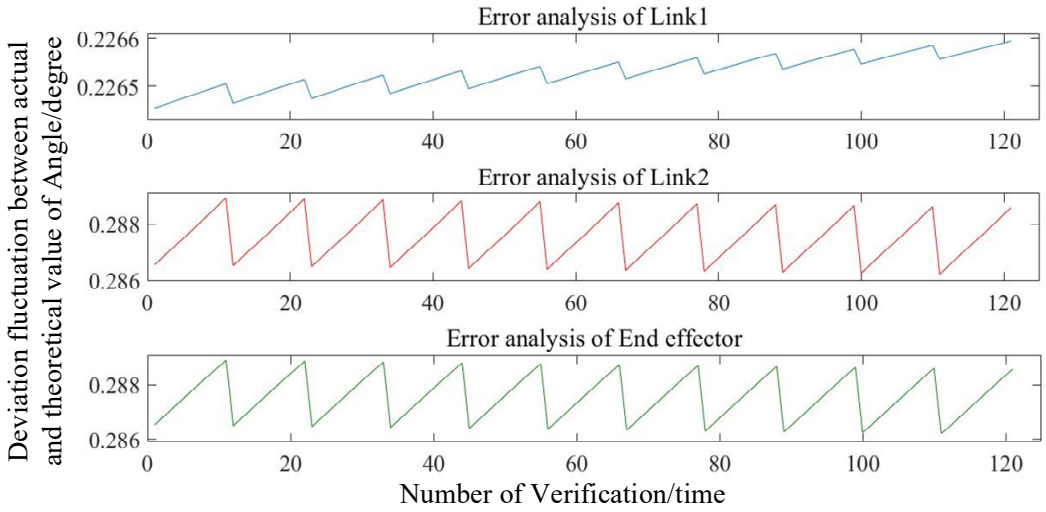

Fig.7 Error analysis between the actual value and the theoretical value of the Angle.

The final endpoints of the actual robotic arm components are summarized in Fig.8. For the end effector, the coordinates of its gripping point are taken as the coordinates of the end effector. The endpoint of Link1 is represented by a red dot, the endpoint of Link2 is represented by a green dot, and the gripping point is represented by an orange dot.

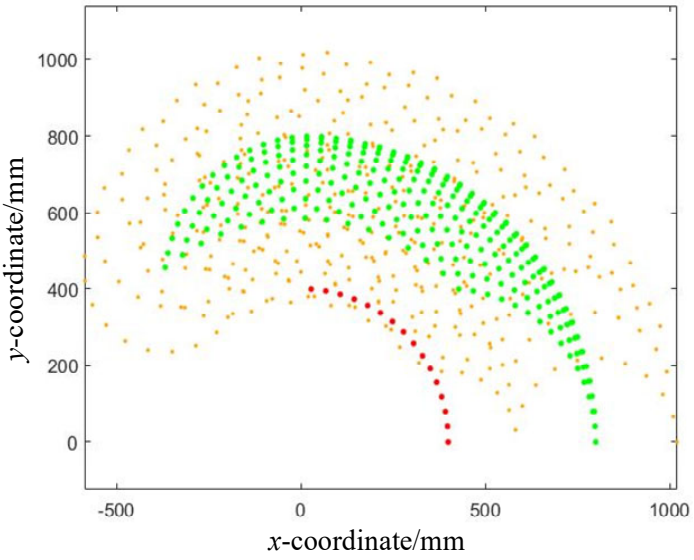

Fig.8 The coordinates of all the actual final points.

Since the three-degree-of-freedom robotic arm has multiple solutions for the coordinates of the end effector after its determination, there may still be fluctuations in the specific $(\theta_1, \theta_2, \theta_3)$. The theoretical angles of the components and the actual control angles will have deviations. Based on the analysis of Fig.7 and Fig.8, for Link1 with a smaller error, the angle error of θ_1 is controlled within 2×10^{-4}. For Link2 and the end effector, which may have larger errors, the angle error fluctuates within 3×10^{-4}. This error is within an acceptable range for this program. Therefore, using a combination of fuzzy control and training ANFIS networks can be considered a reasonable solution for this picking robotic arm system.

To validate the feasibility of the fuzzy control and ANFIS network training scheme, we will consider the actual Y-shaped end effector, as opposed to the simplified linear structure used for analytical convenience. The planes swept by the end effector's two arms represent the harvesting robot's actual working range.

We must consider the maximum working area of the robot, which includes the area swept by the maximum opening Angle of the end effector. The analysis area that you add to the final clamping point will get the maximum working area. The end effector with a maximum open Angle takes a y shape with a 120° Angle between the arms. The lines OA, OB, and OP depict the end effector. The area swept by OA and OB indicates the actual working area of the end effector at the maximum opening Angle. In Fig.9, blue, green, and orange dots are used to mark the possible landing points of O, A, and B respectively.

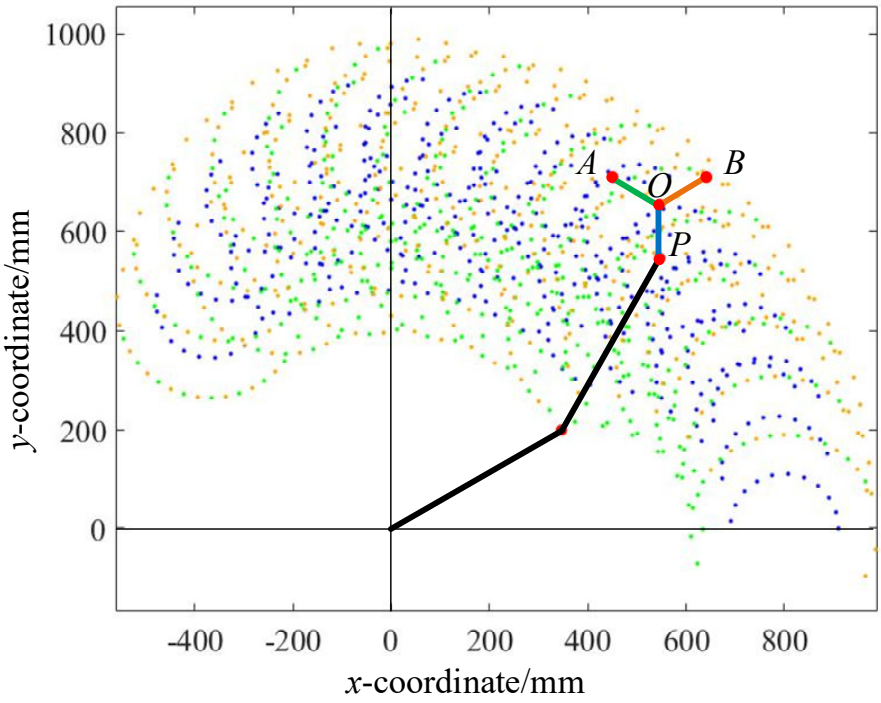

Fig.9 Analysis of landing points for O, A, and B.

To visualize the robot's actual working range, we need to depict the areas swept by the movement of OA and OB, as well as the enveloping surfaces formed by the trajectories of O, A, and B. Fig.10 shows the areas swept by the movement of OA and OB. Combining these areas with the range of the end effector in Fig.8 yields the maximum working range of the robot.

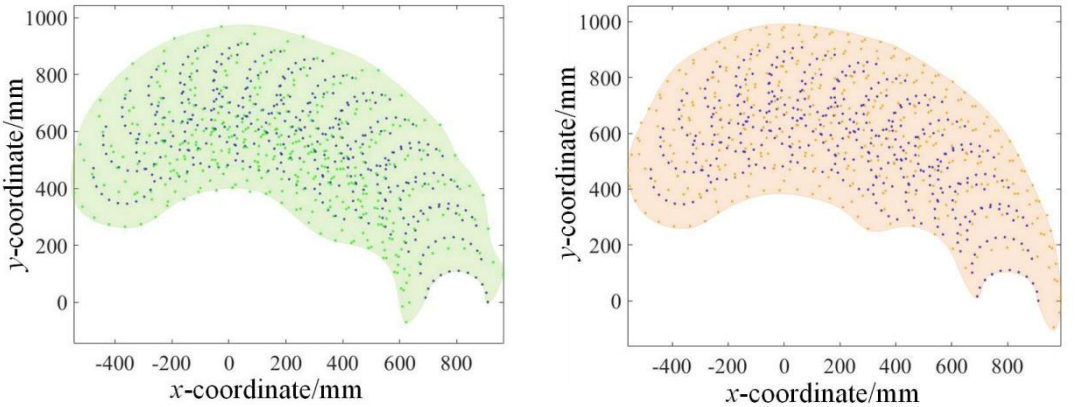

Fig.10 Analysis of gripper claw working range.

To account for the working range of both arms as an additional parameter, we re-analyze the ANFIS network's angle control error by training the network with the (x,y) coordinates and θ at the end of both arms. After considering the gripper's shape, we find that the control results for Link1 and Link2

remain unchanged, and only the fluctuation error between the output value of θ_3 and the theoretical value for either the left or right arm control is considered. The results are shown in Fig.11.

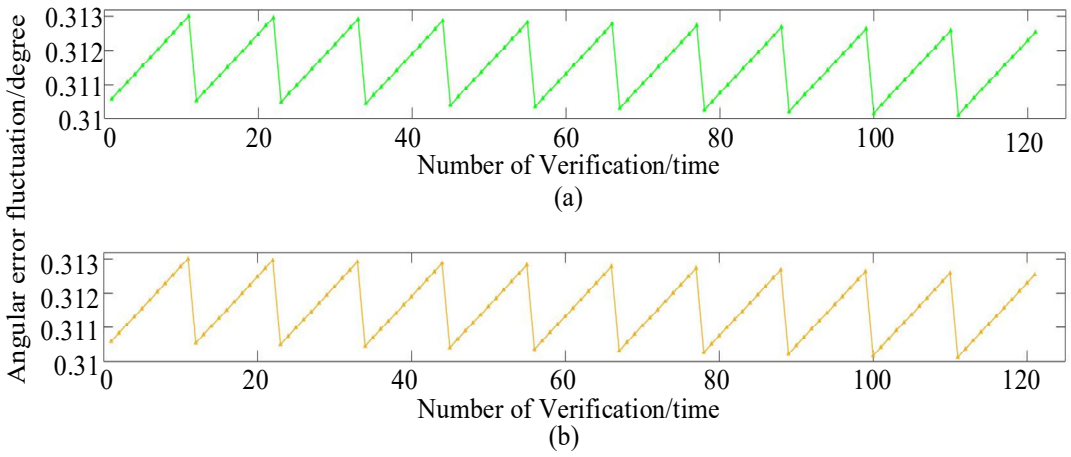

Fig.11 Error analysis considering the shape of the gripper claws. (a) using the coordinates of point A as the training data set. (b) using the coordinates of point B as the training data set.

According to Fig.11, the fluctuation error range of θ_3 control can still be kept within 3×10^{-4}, which validates the previous conclusion that using fuzzy control and ANFIS network is a marvelous method to control this manipulator arm.

4. Conclusion

In the above content, we conducted a kinematic analysis of the manipulator arm and proposed using fuzzy theory and ANFIS network for its control. We also verified the accuracy of this method.

The working range of the manipulator's arm was initially obtained by considering only the end effector's gripping point, as shown in Fig.5. The boundary points of the range are (72.15,1017.45), (-585.50,486.49), (582.20,31.05), and (992.31,183.22). However, after considering the actual gripping range of the end effector, the actual working range is expanded. The boundary points assuming only the maximum opening angle of the gripper are (55.52,998.52),(-557.82,467.86),(965.00,-95.26), and (977.19,70.00).

The ANFIS network's error analysis shows that the error fluctuation between the network output and theoretical values is within 3×10^{-4}. when only considering the end effector's gripping point. After considering the actual shape of the end effector, the effect on the first two links' parameters is negligible, only requiring checking the output error of θ_3. The output error is increased slightly but remains within an acceptable range of 3×10^{-4}. Therefore, using fuzzy theory and ANFIS network for control in practical working conditions is feasible.

The harvesting robot can handle plant and fruit harvesting work that is less than 1 meter in height. Although some fruits may have an actual height lower than the reference plane due to the robot's base height limitation, they can still be harvested considering the claws' actual shape and opening angle. This makes the harvesting robot suitable for shorter plants and fruits while having a smaller size and lower cost compared to other agricultural robots.

References

[1] Emami A, Khaleghian S, Jahromi M M . Design, Analysis, and Simulation of a Pipe-Welding Robot with Fixed Plinth.2015[2023-12-08].DOI:10.48550/arXiv.1501.01930.

[2] Kwantongon J, Suamuang W, Kamata K . A Teaching Demonstration Set of a 5-DOF Robotic Arm Controlled by PLC[J].International Journal of Information and Education Technology, 2022.DOI:10.18178/ijiet.2022.12.12.1772.

[3] Dinger S, Dickens J, Pantanowitz A . Robotic Arm for Remote Surgery.2013[2023-12-08].

[4] Shinohara K. Swimmer simulation using robot manipulator dynamics under steady water[J]. Natural science journals, 2010.DOI:10.4236/NS.2010.29117.

[5] Li K , Huo Y , Liu Y ,et al.Design of a lightweight robotic arm for kiwifruit pollination[J]. Computers and Electronics in Agriculture, 2022.

[6] Yafei Li. Trajectory Tracking Control of Agricultural Picking Robot Arm [J]. Mechanical Engineering and Automation, 2022, (02): 173-175.

[7] Shuo W, Daobilige S, Yiyu J, et al. Fusing vegetation index and ridge segmentation for robust vision-based autonomous navigation of agricultural robots in vegetable farms [J]. Computers and Electronics in Agriculture, 2023, 213.

[8] Li H , Quan L , Guo Y ,et al.Improving agricultural robot patch-spraying accuracy and precision through combined error adjustment[J].Computers and Electronics in Agriculture, 2023.

[9] Moreno J I ,Ouardani D ,Arce C D , et al. Real-Time Hardware-in-the-Loop Emulation of Path Tracking in Low-Cost Agricultural Robots [J]. Vehicles, 2023, 5 (3): 894-913.

[10] Ørum Jens Erik,Tamirat Tseganesh Wubale,Pedersen Søren Marcus. Optimal use of agricultural robot in arable crop rotation: A case study from the Netherlands [J]. Smart Agricultural Technology, 2023, 5.

[11] Wu X ,Bai J ,Hao F , et al. Field Complete Coverage Path Planning Based on Improved Genetic Algorithm for Transplanting Robot [J]. Machines, 2023, 11 (6).

[12] Kumar S, Mohan S, Skitova V . Designing and Implementing a Versatile Agricultural Robot: A Vehicle Manipulator System for Efficient Multitasking in Farming Operations [J]. Machines, 2023, 11 (8).

[13] Agrawal R , Kabiraj K, Singh R . Modeling a Controller for an Articulated Robotic Arm[J].Intelligent Control & Automation, 2012, 3(3):207-210.DOI:10.4236/ica.2012.33023.

[14] Kareemullah H , Najumnissa D , Shajahan M S M ,et al.Robotic Arm controlled using IoT application[J]. Computers and Electrical Engineering, 2023.

[15] Namhyun K ,Daejin O ,JunYoung O , et al. Disturbance-Observer-Based Dual-Position Feedback Controller for Precision Control of an Industrial Robot Arm [J]. Actuators, 2022, 11 (12): 375-375.

[16] Gao J, Chen Y, Li F . Kinect-Based Motion Recognition Tracking Robotic Arm Platform[J]. Intelligent Control and Automation, 2019.

[17] Chuanyang L ,Changhua H ,Jorge A , et al. Dynamics of a modular manipulator with multiple actuation modes for space applications [J]. Mechanism and Machine Theory, 2023, 189.

[18] Ranjan R, Kumar D A . MODELING AND SIMULATION OF ROBOTIC HUMANOID ARM[J].International Journal of Engineering Science & Technology, 2012, 4(6):325-332.DOI:doi:http://dx.doi.org/.